

Electronic Supplementary Information

A novel fluorescent probe for Hg²⁺ detection in a wide pH range and its application in living cell imaging

Jing Xu[‡], Honglin Li[‡], Yanchi Chen, Bing Yang, Qingcai Jiao*, Yushun Yang*, Hailiang Zhu*

State Key Laboratory of Pharmaceutical Biotechnology, Nanjing University, Nanjing, 210023, China.

[‡]Both authors contributed equally to the work.

** Corresponding authors. E-mail addresses: zhuhl@nju.edu.cn; ys_yang@nju.edu.cn; jiaoqc@nju.edu.cn.*

Contents

Supplementary figures and tables	S2
1 UV absorption response of probe XL-1 to Hg ²⁺	S2
2 The UV-Vis titration of Hg ²⁺ towards XL-1	S2
3 The effect of pH on XL-1 and the reaction of XL-1 with Hg ²⁺	S3
4 The response time of probe XL-1 to Hg ²⁺	S3
5 Fluorescence intensity of XL-1 to various metal ions	S4
6 Fluorescence intensity of XL-1 to various amino acids	S4
7 Fluorescence intensity of XL-1 to various anions	S5
8 The effect of water volume fraction on XL-1 sensing Hg ²⁺	S5
9 Cytotoxicity of XL-1 towards A549, HeLa, LO ₂ and CT26 cells	S6
10 NMR spectra of XL-1	S7
11 HRMS spectrum of XL-1 and Product A	S8
12 Comparison between XL-1 and recent small molecule fluorescent Hg ²⁺ sensors	S8

Supplementary figures and tables:

1 UV absorption response of probe XL-1 to Hg^{2+}

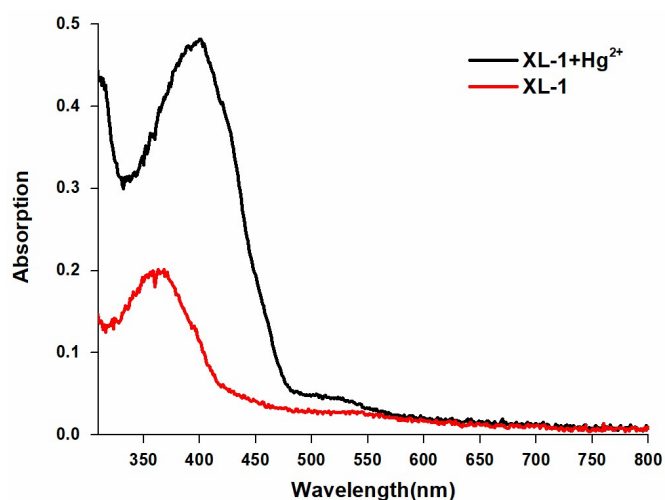


Figure S1. The absorption spectrum of XL-1 (50 μM) and the detecting system (XL-1: 50 μM and Hg^{2+} : 100 μM) in PBS buffer (pH 7.4, 10 mM, 10% DMSO, v/v) at 25 $^{\circ}\text{C}$.

2 The UV-Vis titration of Hg^{2+} toward XL-1.

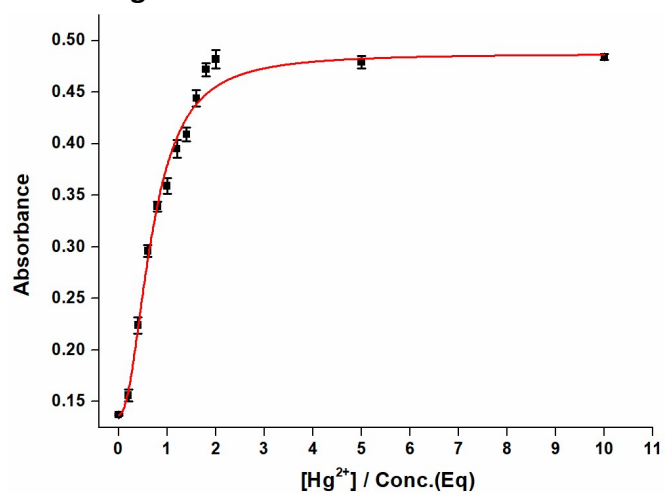


Figure S2. The UV-Vis titration of Hg^{2+} towards XL-1 (50 μM). The Y-axis represents the absorbance at 400 nm corresponding to the absorbance wavelength of the reaction mixture. It agreed with the typical 1:2 binding mechanism.

3 The effect of pH on XL-1 and the reaction of XL-1 with Hg²⁺

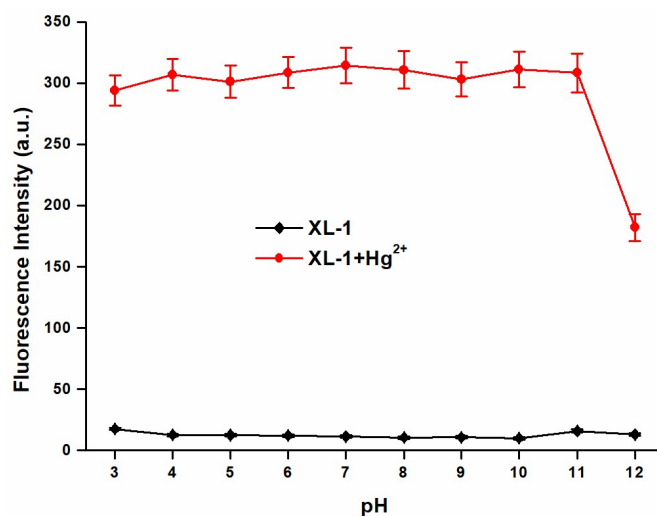


Figure S3. Fluorescence intensity changes of XL-1 (10 μ M) incubated with or without Hg²⁺ (20 μ M) in PBS buffer (10 mM, 10% DMSO, v/v) with different pH values (from 3.0 to 12.0) at 25 $^{\circ}$ C for 1 h (Red: XL-1 + Hg²⁺; Black: XL-1).

4 The response time of probe XL-1 to Hg²⁺

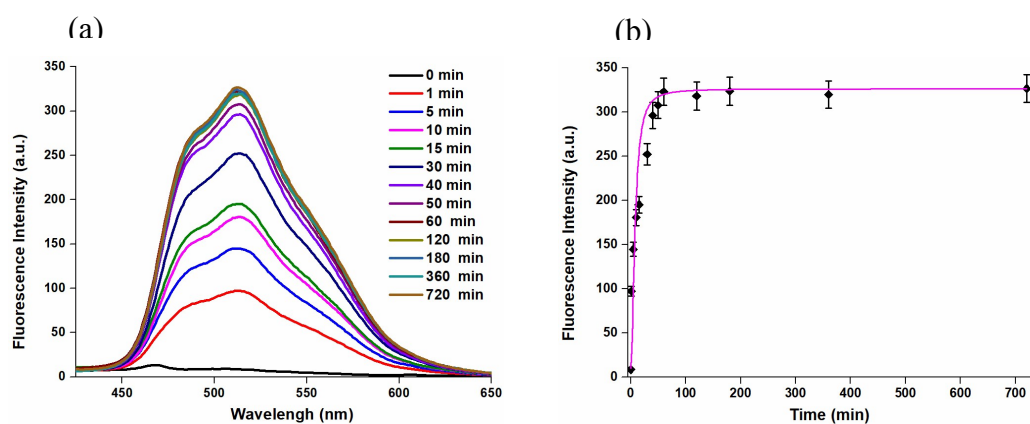


Figure S4. (a) Fluorescence spectra changes of the detecting system in PBS buffer (pH 7.4, 10 mM, 10% DMSO, v/v) at 25 $^{\circ}$ C with time (0-12 h). (b) Relationship between fluorescence intensity and different time points (0, 1, 5, 10, 15, 30, 40, 50, 60, 120, 180, 360, 720 min). The Fluorescence intensity reach the maximum at 60 min. The data represent the mean \pm SD of at least three independent experiments. λ_{ex} = 401 nm, Slit widths 5 nm, Photomultiplier voltage 650 V.

5 Fluorescence intensity of XL-1 to various metal ions

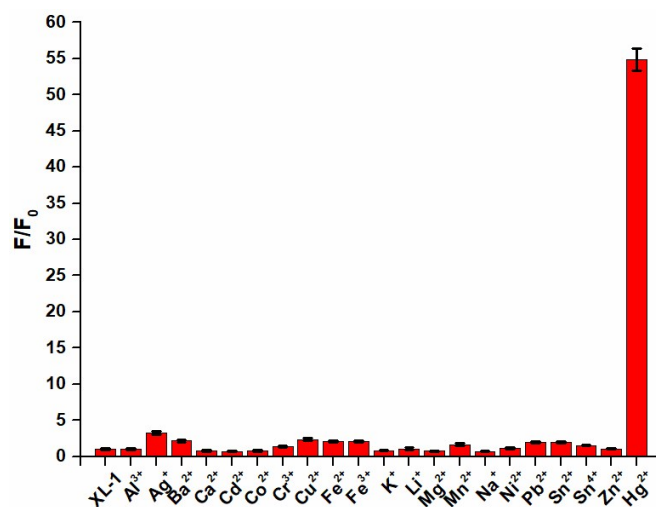


Figure S5. Fluorescence intensity of **XL-1** (10 μ M) in PBS buffer (pH 7.4, 10 mM, 10% DMSO, v/v) at 25 $^{\circ}$ C to various metal ions (20 μ M). The data represent the mean \pm SD of at least three independent experiments. λ_{ex} = 401 nm, Slit widths 5 nm, Photomultiplier voltage 650 V. Incubation time: 1 h.

6 Fluorescence intensity of XL-1 to various amino acids

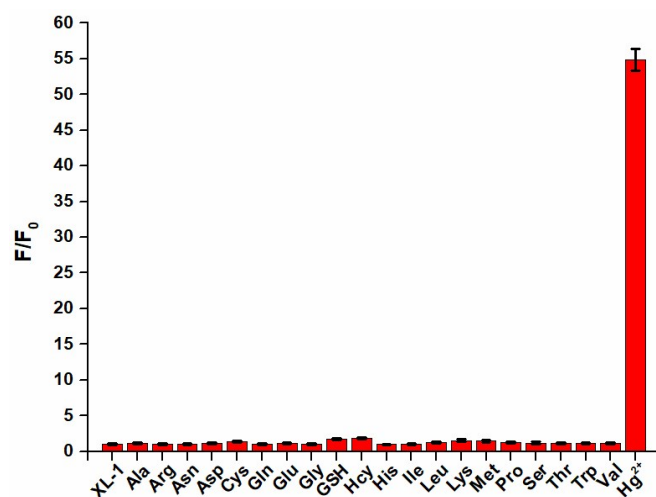


Figure S6. Fluorescence intensity of **XL-1** (10 μ M) in PBS buffer (pH 7.4, 10 mM, 10% DMSO, v/v) at 25 $^{\circ}$ C to various amino acids (200 μ M) (including Hcy and GSH). The data represent the mean \pm SD of at least three independent experiments. λ_{ex} = 401 nm, Slit widths 5 nm, Photomultiplier voltage 650 V. Incubation time: 1 h.

7 Fluorescence intensity of XL-1 to various anions

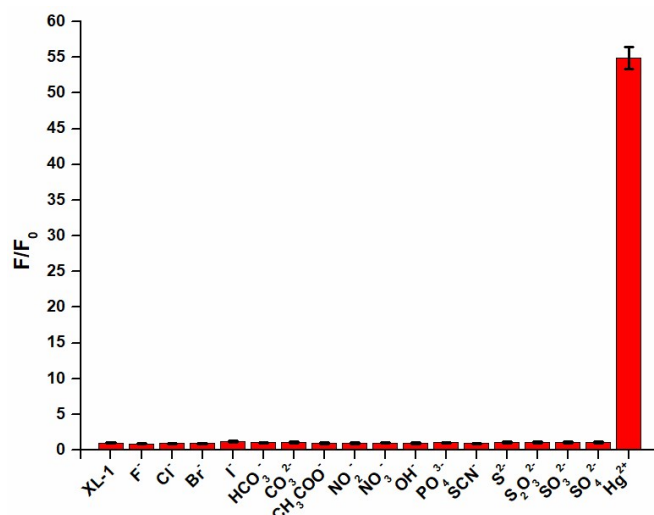


Figure S7. Fluorescence intensity of **XL-1** (10 μ M) in PBS buffer (pH 7.4, 10 mM, 10% DMSO, v/v) at 25 $^{\circ}$ C to various anions (200 μ M). The data represent the mean \pm SD of at least three independent experiments. λ_{ex} = 401 nm, Slit widths 5 nm, Photomultiplier voltage 650 V. Incubation time: 1 h.

8 The effect of water volume fraction on XL-1 sensing Hg²⁺

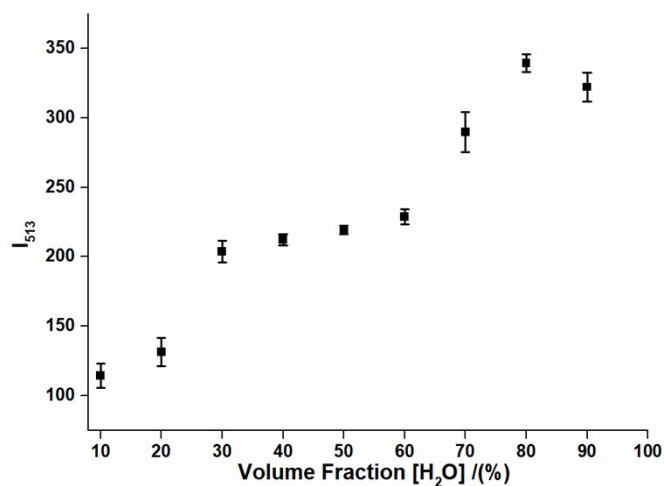


Figure S8. The effect of water volume fraction (10% - 90%) on the probe **XL-1** sensing Hg²⁺. The fluorescence intensity at 513 nm was recorded.

9 Cytotoxicity of XL-1 towards A549, HeLa, LO₂ and CT26 cells

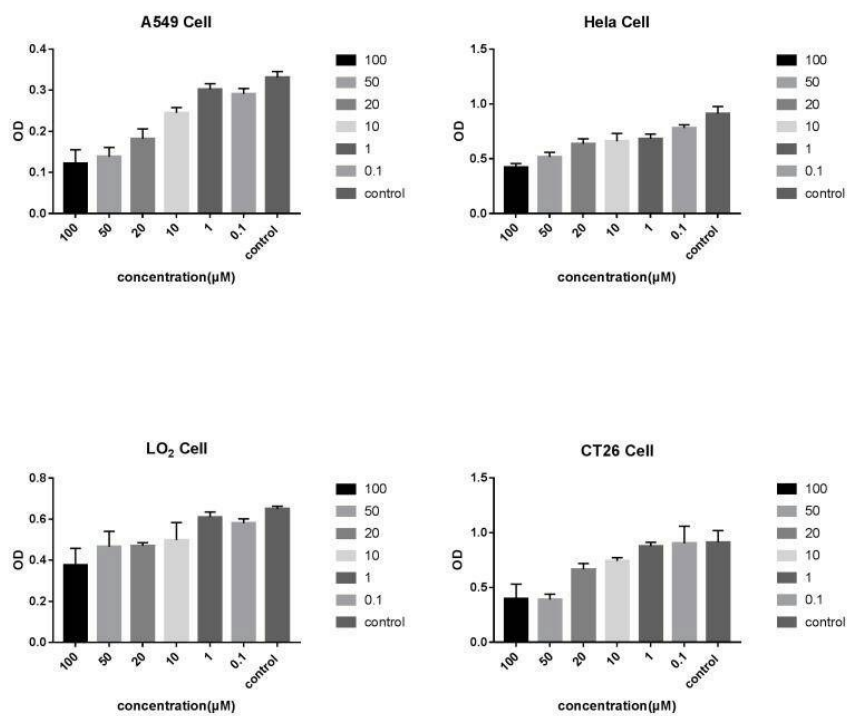


Figure S9. Cell viability of A549 (human alveolar epithelial cell line), HeLa (human cervical cancer cell line), LO₂ (human embryonic liver cell line) and CT26 (mouse colon cancer cells) with different concentrations of **XL-1**.

10 NMR spectra of XL-1

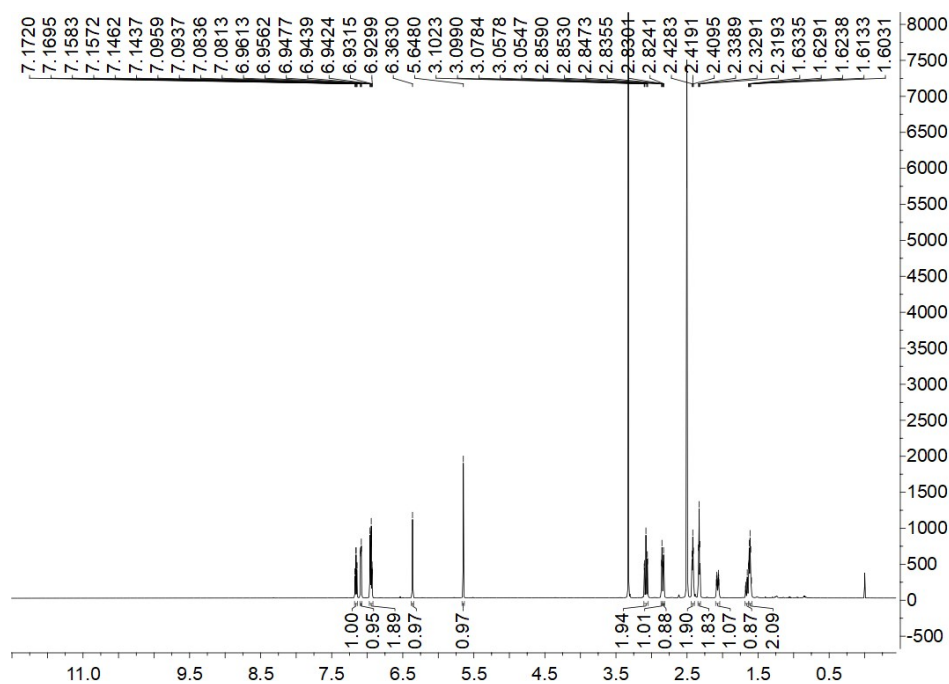


Figure S10. ¹H NMR of compound XL-1 (600 MHz, in DMSO-*d*₆).

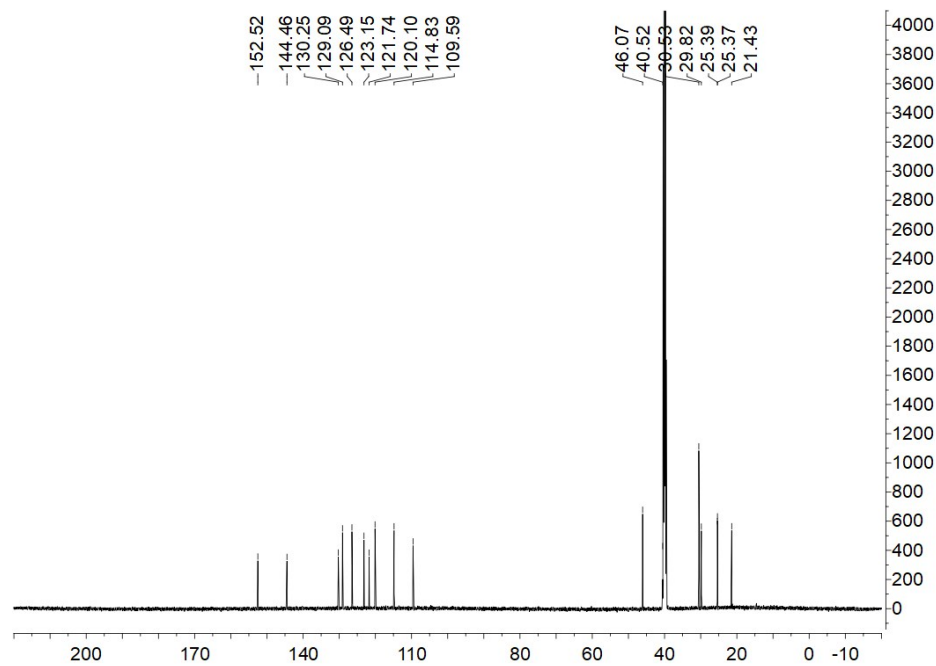


Figure S11. ¹³C NMR of compound XL-1 (150 MHz, in DMSO-*d*₆).

11 HRMS spectrum of XL-1 and Product A

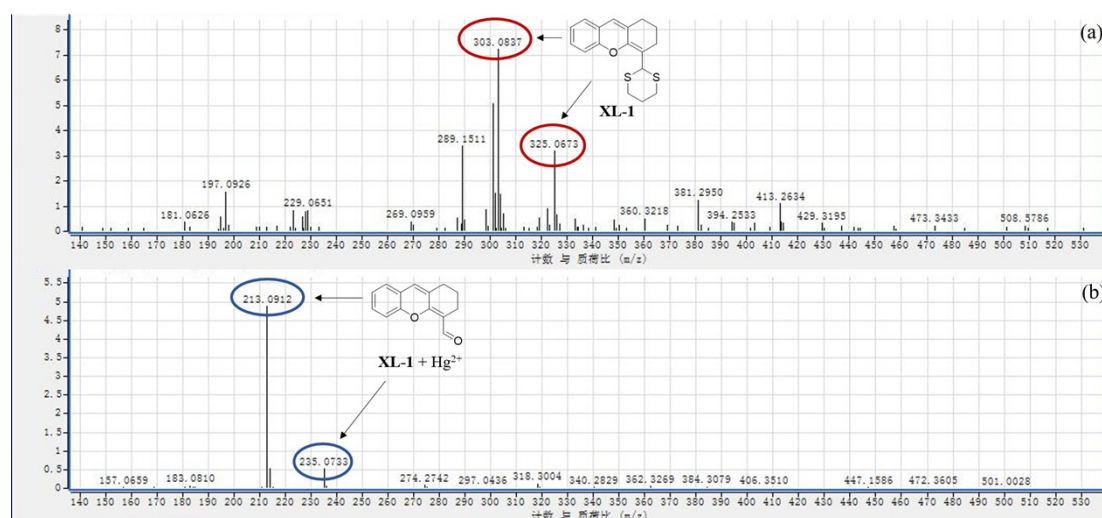


Figure S12. (a) HRMS spectrum of **XL-1**. (b) HRMS spectrum of **Product A**.

12 Comparison between XL-1 and recent small molecule fluorescent Hg²⁺ sensors

Table S1. Comparison between **XL-1** and recent small molecule fluorescent Hg²⁺ sensors.

Sensors	Fluorophore	Range of pH	Sensing mode	EDTA Competition	Steadiness	Toxicity	Application	Selectivity
XL-1	Xanthene	3.0-11.0	Turn on	Done	>12h	Low	Cell imaging	High
Ref 18	Coumarin	4.0-7.0	Turn on	NG	NG	NG	Real water sample	High
Ref 19	Coumarin	6.5-9.0	Turn on	NG	NG	Low	Cell imaging	High
Ref 24	Rhodamin	4.0-10.0	Ratio	NG	NG	Low	Cell imaging	Not good
Ref 25	Rhodamin	3.5-4.5	Turn on	NG	NG	NG	NG	Except Cu ²⁺
Ref 29	Benzothiazole	3.0-5.0	Turn on	NG	NG	NG	Waste water	High
Ref 34	Pyrene	3.0-7.4	Turn on	NG	NG	NG	Cell imaging	Not good
Ref 37	Naphthalene	7.5-10.0	Turn off	NG	NG	NG	Real water sample	Not good
Ref 38	Anthracene	7.0-9.0	Turn on	NG	NG	Low	Cell imaging	High
Ref 39	BODIPY	5.0-8.0	Turn on	NG	NG	Low	In vivo imaging	Except Al ³⁺
Ref 40	BODIPY	7.0-12.0	Turn off	Done	NG	Low	Cell imaging	Not good

NG means Not Given; For each property the top class sensors were labeled in blue.